

---

## NUMERICAL SIMULATION OF 4-DIGIT INCLINED NACA 00XX AIRFOILS TO FIND OPTIMUM ANGLE OF ATTACK FOR AIRPLANE WING

*Haci SOGUKPINAR\**

---

Received: 26.02.2016; revised: 05.12.2016; accepted: 28.02.2017

**Abstract:** In this paper, numerical analysis was conducted by using the SST turbulence model for inclined NACA 0008, 0009, 0010, 0012, 0015, 0018, 0021, 0024 airfoils. Aerodynamic numerical analysis of NACA 0012 airfoil was compared with the previously made experimental results in terms of pressure and lift coefficient. The theoretical data were found to be fully compatible with experimental results. Then, by simulating other airfoils using the same methods lift, drag, lift to drag ratio and the pressure coefficient were calculated and compared with the angle of attack 0-14 degrees. According to the calculations, lift coefficient of NACA 0008-0012 airfoil shows similar behaviors. With the increasing of the airfoil thickness increment in the lift coefficient decreases for NACA 0015-0024 airfoils. Pressure coefficients were also calculated for NACA profiles with angle of attack 10°. Pressure coefficients over the airfoil decrease from leading edge toward the trailing edge but in the lower part it increases. With the increasing of the airfoil thickness pressure coefficient decreases more slowly at the upper part but increases more rapidly at the lower.

**Key words:** Airfoil, NACA 4 series, COMSOL, numeric analysis, airfoil simulation

### Uçak Kanatlarında En İdeal Hücüm Açısını Bulmak İçin 4 Rakamlı NACA 00xx Kanat Profillerinin Nümerik Analizi

**Öz:** Bu çalışmada SST türbülans modeli kullanılarak 4 rakamlı NACA kanat profillerinden 0008, 0009, 0010, 0012, 0015, 0018, 0021, 0024 nümerik olarak analiz edilmiştir. NACA 0012 kanat profili deneysel verilere sahip olduğu için önce bu kanat kesiti simüle edilip deneysel verilerle kaldırma kuvvet ve basınç katsayısı bakımından kıyaslanmıştır. Bu çalışmada yapılan teorik hesaplamalar ile deneysel verilerin tam olarak uyumlu olduğu gözlemlenmiştir. Daha sonra aynı yöntem kullanılarak diğer kanat profilleri simüle edilerek kaldırma kuvveti, sürüklenme kuvveti ve profil yüzeyindeki basınç katsayıları ve kaldırma kuvvet katsayısının sürüklenme kuvvet katsayısına oranı hesaplanarak farklı hücüm açıları için kıyaslamalar yapılmıştır. Yapılan hesaplamalara göre NACA 0008-0012 profilleri benzer aerodinamik özellik göstermektedir. Kanat profillerinin kalınlığı arttıkça lift katsayısının azaldığı gözlemlenmiştir. Ayrıca her profil için 10 derecelik hücüm açısında basınç katsayıları hesaplanmış ve profil kalınlığı arttıkça profilin üst kısmındaki basınç katsayısı daha yavaş azalırken alt kısımda daha hızlı bir şekilde artmıştır.

**Anahtar Kelimeler:** Kanat profili, NACA 4 serisi, COMSOL, sayısal analiz, kanat simülasyonu

## 1. INTRODUCTION

NACA airfoil is designed generally for aircraft. Then, some designed airfoils have been also used in wind turbines. First-designed 4 and 5 digit number NACA airfoils are expressed in terms of analytical equations and can be obtained with the help of it. Later designed airfoil has more complex structure and can obtain with the aid of theoretical calculations.

---

\* Department of Energy Systems Engineering, Faculty of Technology, University of Adiyaman, Adiyaman 02040, Turkey

Corresponding Author: H. Soğukpınar (hsogukpınar@adiyaman.edu.tr)

Xu et al. (2015) conducted numerical simulations of NACA 4409, 4412, 4415 and 4418 series and lift and drag coefficients for the NACA 4415 airfoil were calculated using k- $\omega$  and SST turbulence models. With this study they compared experimental data with theoretical one, the accuracy of the computational fluid dynamics was observed. When the angle of attack passed 9 degree, increment in the lift coefficient was very slow for NACA 4418 airfoil. NACA 4412 airfoil calculations showed that the lift coefficient increased more quickly with respect to others. NACA 4412 airfoil showed the maximum lift coefficient increment and second one was 4415 airfoil. Thumtha et al. (2009) and Aniket et al. (2015) conducted numerical simulations of S809 airfoil. Studies were conducted in calculating the lift coefficient for different angles of attack and obtained results were compared with the NREL experimental data. The ideal angle of attack was determined by using the lift coefficients obtained for different angles. k- $\omega$  turbulence model was used for numerical analysis. Also Aniket et al. (2015) examined numerical simulations of the modified NACA 0006 airfoil of Selig S1123, Eppler E423 and FX 74-CL5-140. Studies confirmed the existence of high lift coefficient Selig S1123 airfoil. Zanotti et al. (2014) made numerical 2D/3D modeling of NACA 23012 airfoil and results were compared with experimental data. Studying with 3D modeling to examine the wing performance by the deep stall was found to be the most appropriate modeling with respect to 2D. Guoqing et al. (2014) made numerical simulation of NACA 0015 airfoil with k- $\omega$  shear stream transport turbulence model and numerical simulations were performed to investigate the effects of synthetic jet control on separation and stall over rotor airfoils. Then, parametric analyses were conducted for an OA213 rotor airfoil for same reason. Rostamzadeh et al. (2014) made the numerical analysis of NACA 0021 airfoil. With the study, It was found that a skew-induced mechanism accounted for the formation of streamwise vortices whose development accompanied by flow separation in delta-shaped regions near the trailing edge. Mashud et al. (2014) made the numerical simulations of NACA 0015 airfoil using k- $\omega$  turbulence models and lift coefficient was calculated and compared with experimental results.

In this study, numerical simulations was performed using the SST turbulence model for NACA 0008, 0009, 0010, 0012, 0015, 0018, 0021, 0024 airfoil. While only one or two airfoils were examined in other studies but here 8 airfoils are investigated and compared with experiment. NACA 0012 airfoil simulation results were compared with Ladson (1988) experimental lift coefficient data and Gregory and O'Reilly (1970) experimental pressure coefficient data. Numerical simulation results show full compliance with the experimental data. Other simulations were carried out using the same method with NACA 0012. Then the coefficient of lift, drag and pressure were compared for NACA 0008, 0009, 0010, 0012, 0015, 0018, 0021, 0024 airfoils and the effect of the thickness of airfoil on the lift, drag and pressure coefficients were investigated. According to numerical calculations with the increasing of the airfoil thickness, increment in lift coefficient decreases. Pressure coefficient at the top of the airfoil decreases from leading to the trailing edge but at the lower side it increases and pressure coefficient decreases slowly at the upper side and increases more rapidly at the lower one.

## 2. COMPUTATIONAL METHOD

NACA airfoil shapes are expressed by numerical figures. In these series, NACA 4 series are the first design airfoils. Putting the numbers in the numeric code on the equation, geometrical characteristics of the airfoil is determined. The first digit in the 4-digit NACA series determines the maximum amount of curvature and takes place in steps as the percentage amount of the chord length. The second digit represents location of the maximum amount of curvature of the airfoil from the leading edge as a percentage. The last two digits specify the maximum thickness of the airfoil as a percentage of chord length. For NACA 2415 airfoil, the maximum curvature is 2% of the chord, starting from 40% from the leading edge and maximum thickness of airfoil is 15% of chord length. If the first two digits of the NACA are 00, it has a symmetrical structure and does not have a curvilinear geometry.

For NACA 0012 airfoil, the maximum thickness is equal to 12% chord length with symmetrical geometry. In symmetrical NACA airfoil geometry is expressed by equation (1) (Eastman, 2015).

$$y_t = 5tc \left[ 0.2969 \sqrt{\frac{x}{c}} + (-0.1260) \left(\frac{x}{c}\right) + (-0.3516) \left(\frac{x}{c}\right)^2 + 0.2843 \left(\frac{x}{c}\right)^3 + (-0.1015) \left(\frac{x}{c}\right)^4 \right] \quad (1)$$

Here,  $c$  is chord length,  $x$  is coordinate value between 0- $c$ ,  $y_t$  is half thickness of airfoil for a given  $x$  value,  $t$  is the percentage of the maximum thickness.

Before US National Advisory Committee for Aeronautics (NACA), airfoil design had been done randomly. Past experience would have been taken into account in the design. Since the early 1930s, airfoil design had been made by NACA. Different airfoils were designed by NACA (new name is NASA) and were performed wind tunnel tests at different concentrations. High Reynolds numbers were used in the experimental tests. The main reason of the experimental test was to obtain the optimum airfoil shape for the required application. The first experimental tests were conducted by NACA, limited to the 68 airfoil in the series. However, during test, some other supporting airfoils were also used. Design and wind tunnel test results were plotted in the form of reports and it has been published. General shape of the airfoil is given in Fig. 1.

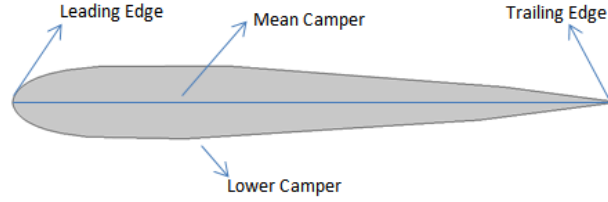


**Figure 1:**  
*Cross-section of airfoil.*

In this study, SST turbulence model was used together with a Parametric Sweep for the angle of attack to compute the different flows on a Mapped Mesh. To combine superior behavior of k- $\omega$  model close to the Wall region with the superior strength of the model, SST (Shear Stress Transport) model was developed by Menter (1994). SST model is expressed in terms of k and  $\omega$  with equation (2) and (3) (COMSOL, 2015).

$$\rho \frac{\partial k}{\partial t} + \rho u \cdot \nabla k = P - \rho \beta_0^* k \omega + \nabla \cdot ((\mu + \sigma_k \mu_T) \nabla k) \quad (2)$$

$$\rho \frac{\partial \omega}{\partial t} + \rho u \cdot \nabla \omega = \frac{\rho \gamma}{\mu_T} P - \rho \beta \omega^2 + \nabla \cdot ((\mu + \sigma_\omega \mu_T) \nabla \omega) + 2(1 - f_{v1}) \frac{\rho \sigma_\omega \omega^2}{\omega} \nabla \omega \cdot \nabla k \quad (3)$$

Where, P is the static pressure and can be represented with the equation (4).

$$P = \min(P_k, 10\rho\beta_0^* k\omega) \quad (4)$$

Here,  $P_k$  production term and it is expressed with equation (5).

$$P_k = \mu_T \left( \nabla u : (\nabla u + (\Delta u)^T) - \frac{2}{3} (\nabla \cdot u)^2 \right) - \frac{2}{3} \rho k \nabla \cdot u \quad (5)$$

Turbulence viscosity is expressed with equation (6).

$$\mu_T = \frac{\rho a_1 k}{\max(a_1 \omega, S f_{v2})} \quad (6)$$

Where, S is the characteristic magnitude of the mean velocity gradients and is expressed with the help of equation (7)

$$S = \sqrt{2S_{ij}S_{ij}} \quad (7)$$

The interpolation functions  $f_{v1}$  and  $f_{v2}$  are represented with the equation (8) and (9)

$$f_{v1} = \tanh \left( \min \left[ \max \left( \frac{\sqrt{k}}{\beta_0^* \omega l_\omega}, \frac{500\mu}{\rho \omega l_\omega^2} \right), \frac{4\rho\sigma_\omega k}{\max(\frac{2\rho\sigma_\omega \omega^2}{\omega} \nabla \omega \cdot \nabla k, 10^{-10}) l_\omega^2} \right] \right)^4 \quad (8)$$

$$f_{v2} = \tanh \left( \max \left( \frac{\sqrt{k}}{\beta_0^* \omega l_\omega}, \frac{500\mu}{\rho \omega l_\omega^2} \right)^2 \right) \quad (9)$$

Where,  $l_\omega$  is the distance to the closest wall. For SST, default model constants are given by (COMSOL, 2015),

$$\beta_1 = 0.075, \gamma_1 = \frac{5}{9}, \sigma_{k1} = 0.85, \sigma_{\omega1} = 0.5, \beta_2 = 0.0828, \gamma_2 = 0.44, \sigma_{k2} = 1.0, \sigma_{\omega2} = 0.856, \beta_0^* = 0.09, \sigma_1 = 0.31$$

The computational conditions are as shown in Table 1.

**Table 1. Computational condition**

Density	1.2043 kg/m <sup>3</sup>
Wind speed	50 m/s
Angle of attack (Deg)	0.2,4,6,8,10,12,14
Turbulent kinetic energy	4.1840E-7 m <sup>2</sup> /s <sup>2</sup>
Specific dissipation rate	2.7778 1/s
Chord lengths	1.8 m
Temperature	193 K
Reference pressure	1 atm
Reference Length	0.2 m
Reynolds number	6.00E+06

In this study, wind speed 50 m/s was set (Mack number 0.15) and adopted as incompressible flow. Flow over the boundary conditions of airfoil was assumed to be turbulence because Reynolds number was in the range of million. Air flowing over the airfoil surface was arranged to be inclined. Calculated distance was taken 100 times of the chord length from the leading edge of airfoil to the inlet and taken 200 times from trailing edge to open boundary. Here, it was the purpose to minimize the impact of the boundary region in calculation. A computational domain is given in Figure 2. Closed-up of airfoil section is given in Figure 3 to be used for numerical calculations. No slip condition is applied on the surface of the airfoil.

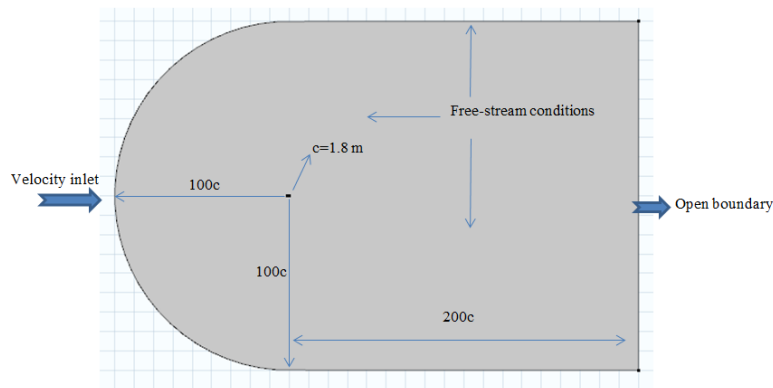


**Figure 2:**  
*Computational domain and boundary condition*

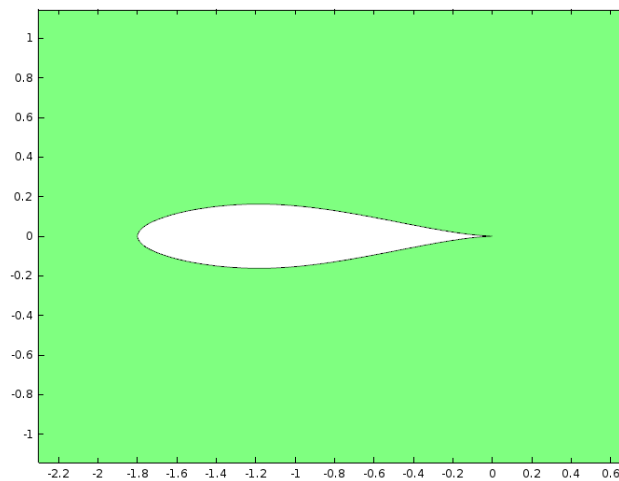


**Figure 3:**  
*Closed-up of airfoil section*

Computational grids were generated using COMSOL software. c-shaped section was applied to eliminate distortions in boundary region. For the calculation of the mesh, 4 different parts of the mesh was applied separately to each section in Figure 4.

Very sparse or too dense grid may cause high error in calculation and values were selected to be compatible with the experimental data. The same intensity in the mesh geometry for all other airfoils were created. Mesh distribution around the airfoil is given in Figure 4.

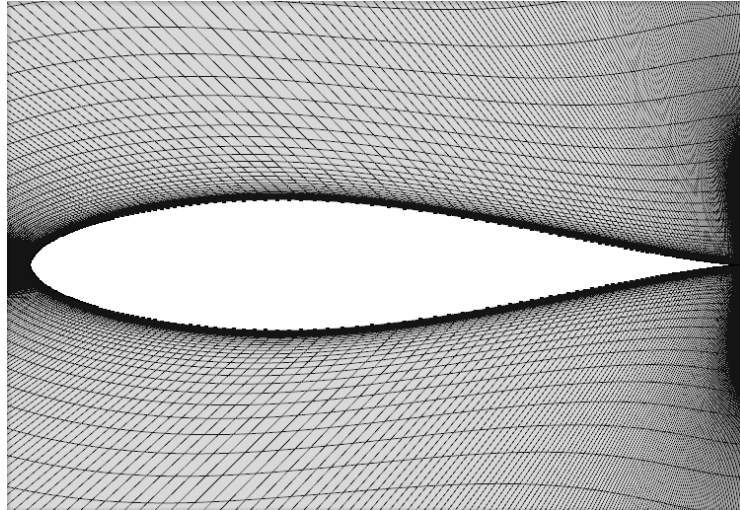


**Figure 4:**  
Mesh distrubution around the airfoil

### 3. RESULTS AND DISCUSSION

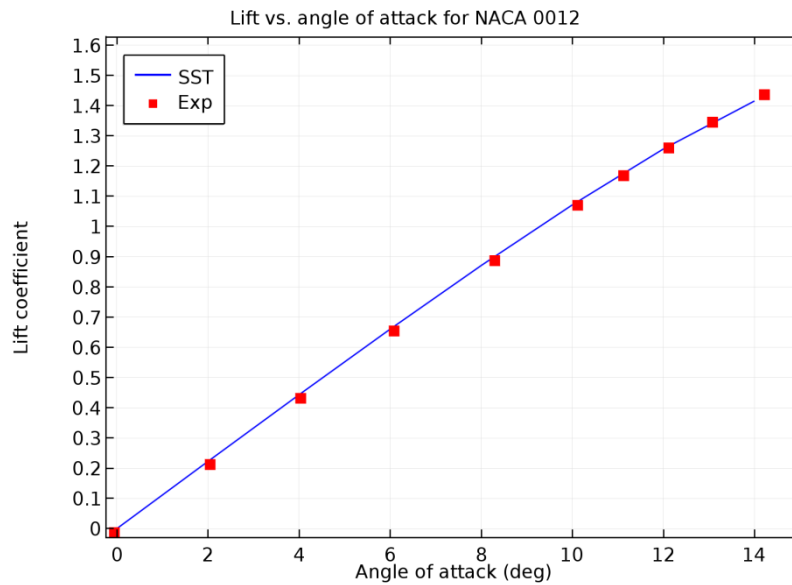
This study was conducted using COMSOL 4.3b simulation software for NACA airfoil 00XX series. The SST model was used for numerical analysis and flow around the airfoil was assumed to be turbulent. Airfoil used in this study has symmetrical structure and the only difference between the airfoil is thickness. The lift, drag and pressure coefficient were calculated using the same method and graphs were generated for lift and drag coefficient, lift to drag ratio and pressure coefficient. Lift coefficient was calculated by equation (9).

$$C_L(\alpha) = \int (c_p(s)/c)(n_y(s) \cos(\alpha) - n_x(s) \sin(\alpha)) ds \quad (9)$$

Here,  $c_p$  pressure coefficient and is expressed with the equation (10).

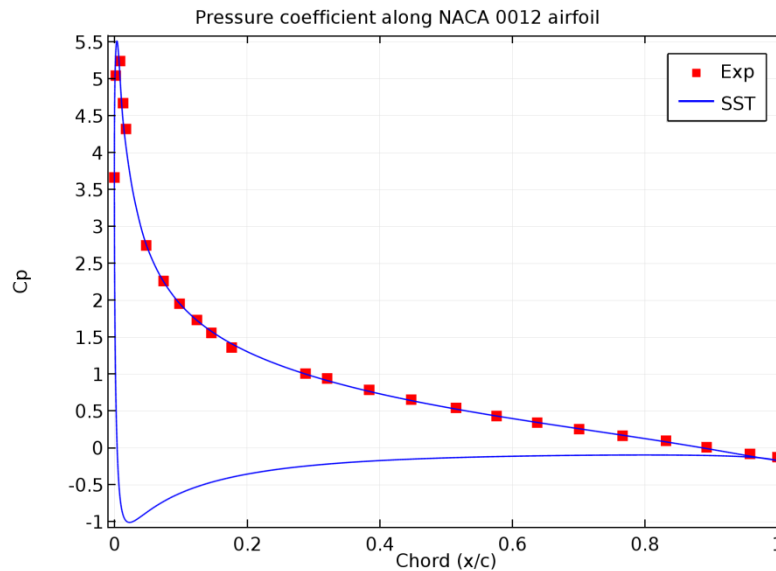
$$c_p(s) = \frac{p(s) - p_\infty}{1/2 \rho_\infty U_\infty^2} \quad (10)$$

At the beginning, numerical analysis of the airfoil NACA 0012 was performed. Then obtained results were compared with previously conducted experimental work for this airfoil (Ladson, 1988). Theoretical data obtained in this study was found to be fully compatible with the experimental data. Computational and experimental result for NACA 0012 airfoil is given in Figure 5.



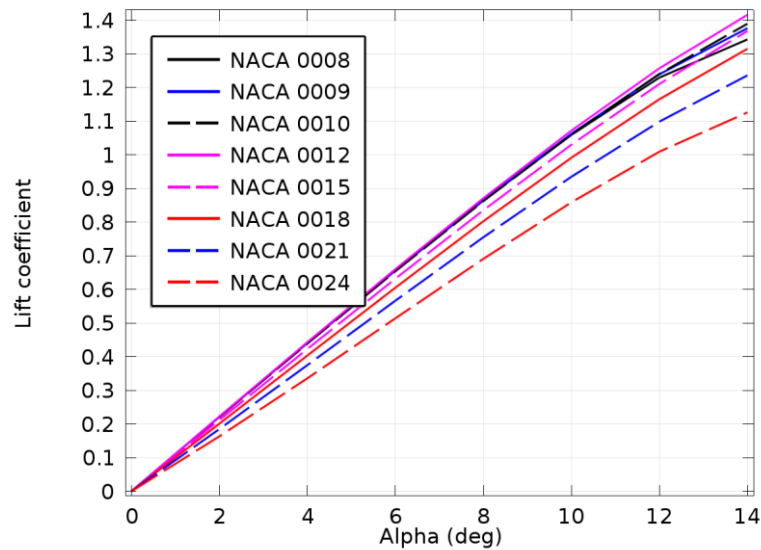
**Figure 5:**  
Computational and experimental result for lift coefficient for NACA 0012.

This study was conducted between 0-14° and shows one-to-one overlap with experimental results as shown in Figure 5. Pressure coefficient for the low pressure region of NACA 0012 airfoil was measured experimentally before (Gregory, 1970). Also in this study, pressure coefficient formed around of NACA 0012 airfoil ( $\alpha = 10^\circ$ ) were calculated and compared with experimental data. Calculated pressure coefficient (line) along the airfoil with the experimental data (dots) is given in Figure 6.



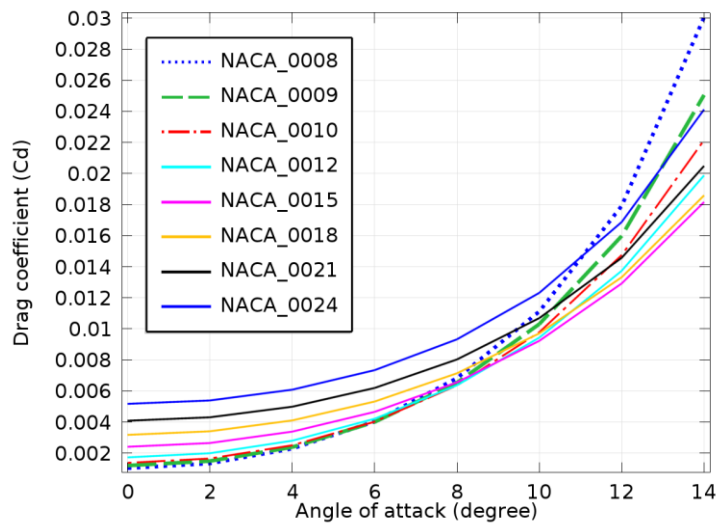
**Figure 6:**  
Computational and experimental results for pressure coefficient around airfoil NACA 0012

The lift and pressure coefficient calculated for the NACA 0012 airfoil were found to be full compliance with experimental data. Then using the same methods lift and pressure coefficient were calculated for NACA 0008, 0009, 0010, 0015, 0018, 0021, 0024 airfoil and graphs were generated. Lift coefficient vs. angle of attack is shown in Figure 7.



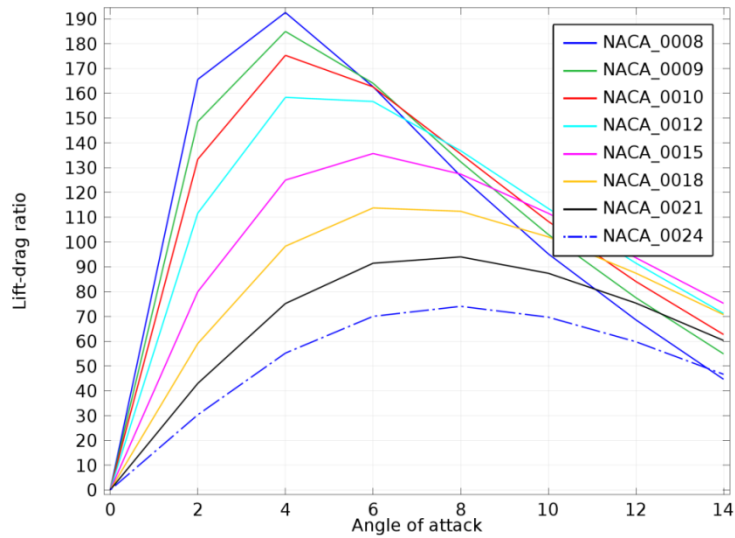
**Figure 7:**  
Computational result for lift coefficient vs. angle of attack.

According to Figure 7, the lift coefficient steadily increases with angle from 0 to 14 degrees. With the increasing relative thickness, the increment in lift coefficient decreases. The lift coefficient at zero angles is slightly greater than zero. NACA 0008 airfoil is the thinnest airfoils analyzed in this study and the lift coefficient increment is similar to NACA 0008-0012 airfoils.



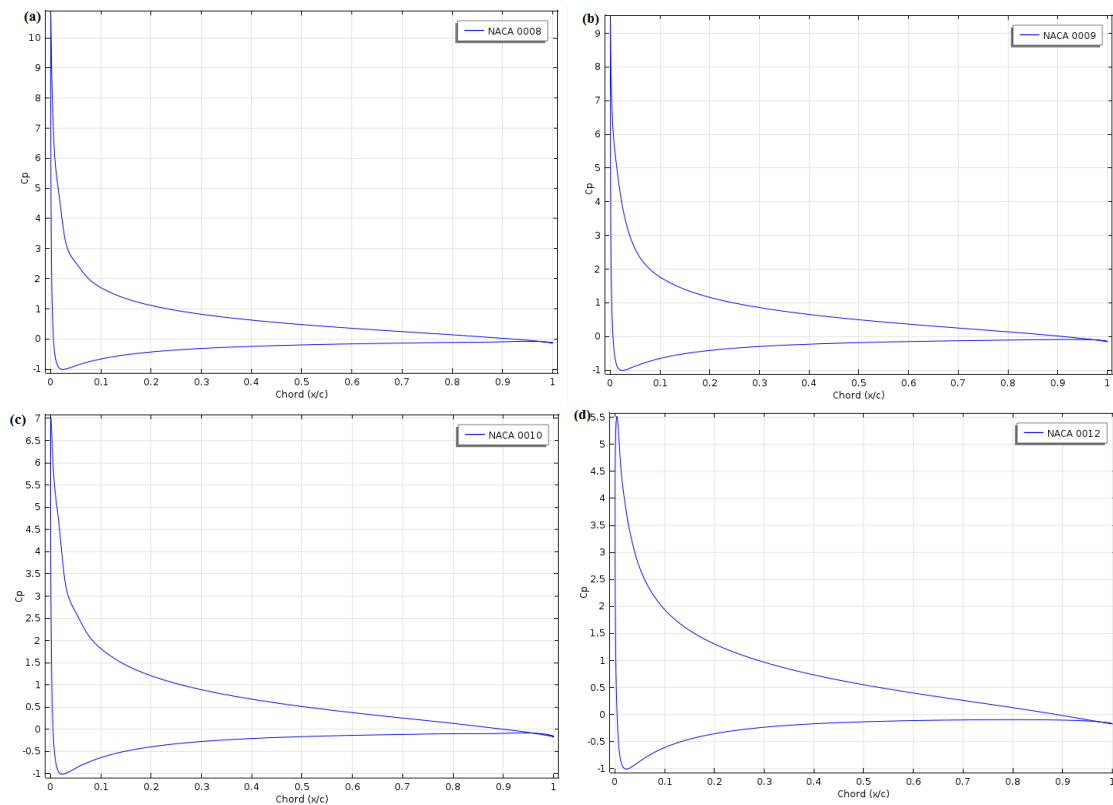
**Figure 8:**  
Computational result for drag coefficient vs. angle of attack

Drag coefficient were calculated, analyzed and presented in Figure 8. According to Figure 8 drag coefficients increase with the increasing thickness of airfoil. Drag coefficient increment is proportional to the thickness at the lower angle but it is not after 6 degree. NACA 0008 airfoil shows the highest increment after 11 degree and NACA 0015 shows lowest. Figure 9 shows the lift-drag ratio of NACA profiles with respect to angle of attack. For the airfoil from 0008 to 0012, they show maximum lift to drag ratio at the angle of 4 degree. Maximum lift to drag ratio angle increases with the increasing of relative thickness after 4° and it becomes maximum at the angle of 8° for NACA 0024. Lift-drag ratio becomes maximum around 5-8 degree and after that start to decrease for all airfoils.



**Figure 9:**  
Lift to Drag ratio versus angle of attacks.

Pressure coefficients formed around airfoils are given in Figure 10 for angle of attack  $10^\circ$ . The pressure formed in the upper surface for all airfoils decreases rapidly from leading to trailing edge but in the lower side it increases. With the increasing of relative thickness, pressure coefficient decreases more slowly in the upper side but increases rapidly in the lower side. Pressure difference increases with increasing airfoil thickness when compared upper and lower surfaces. However, with the increasing relative thickness, the drag coefficient also increases and lift coefficient increment is not proportional to the thickness of airfoil. If drag coefficient didn't increase with the thickness of airfoil, thick airfoil would have a maximum lift coefficient.



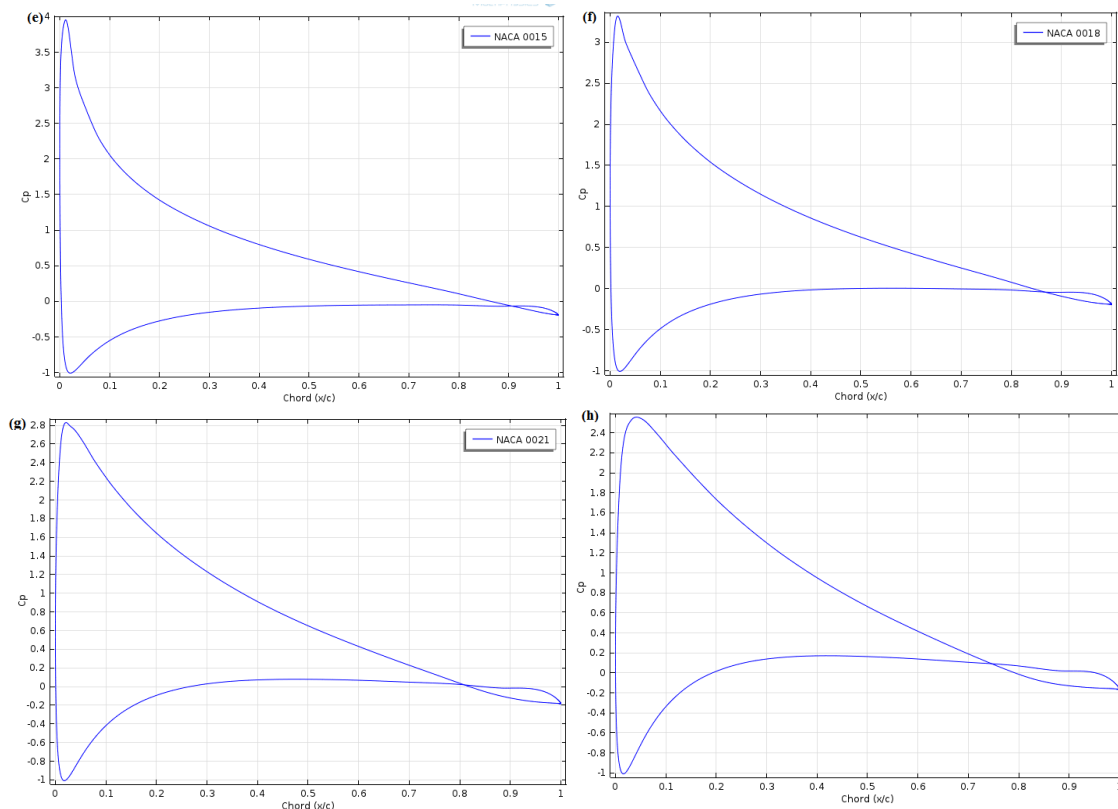


**Figure 10:**

*Pressure coefficient of airfoils with different relative thickness at the angle of attack  $10^\circ$  (a) NACA0008, (b) NACA0009, (c) NACA0010, (d) NACA0012, (e) NACA0015, (f) NACA0018, (g) NACA0021, (h) NACA0024*

#### 4. CONCLUSION

In this study, numerical simulations of NACA 00XX airfoils was conducted using the SST turbulence model. First, theoretical results for the NACA 0012 airfoil were compared with previously made experimental data. Theoretical calculation results were found to be fully compatible with experimental data. Then the other NACA 00XX airfoils were simulated in the same way with the NACA 0012. The effect of the airfoil thickness on the lift and drag coefficient were compared with the angle of attack 0-14 degrees. With the increasing relative thickness, lift coefficient of NACA 0008-0012 airfoils shows similar trend and increment in the lift coefficient decreases gradually from 0015 to 0024. In addition, the pressure coefficients are calculated for NACA 0012 airfoil and is compared with experimental data. The theoretical data are found to be fully compatible with experimental results and using the same methods the pressure coefficients are calculated and graphics are created for other airfoils. The pressure coefficient formed in the top surface of the airfoil shows decrement gradually from leading to trailing edge. With the increasing of relative airfoil thickness from 0008 to 0024, pressure coefficient decreases more slowly in the top surface. The pressure coefficient at the lower surface shows increment from leading to trailing edge and with the increasing of relative thickness it increases faster.

#### ACKNOWLEDGMENT

I thank Middle East Technical University, allowing me to do this work in there with their facility.

#### NOMENCLATURE

$C_p$	Pressure coefficient
$C_L$	Lift coefficient
$P$	Static pressure

$P_{\infty}$	Free stream pressure
$U_r$	Relative velocity
$U_{\infty}$	Free stream velocity (wind velocity)
$u$	Velocity field x component
$v$	Velocity field y component
$c$	Airfoil chord
$t$	Percentage of the maximum thickness
$k$	Turbulence kinetic energy
$l_{ref}$	Reference length scale
$\varepsilon$	Turbulence dissipation rate
$\omega$	Rotational velocity
$\rho$	Density
$\rho_{\infty}$	Freestream density
$\mu$	Dynamic viscosity
$\mu_{eff}$	Effective dynamic viscosity
$\alpha$	Angle of attack
NACA	National Advisory Committee for Aeronautics
NASA	National Aeronautics and Space Administration

## REFERENCES

1. Eastman NJ, Kenneth EW, and Robert MP. (1935). The characteristics of 78 related Airfoil Sections from test in the variable-density wind tunnel. NACA Report no: 460.
2. Xu Z, Wei L, Hailong L. (2015) Numerical simulation of the effect of relative thickness on aerodynamic performance improvement of asymmetrical blunt trailing-edge modification. *Renewable Energy*, 80: 489-497. doi:10.1016/j.renene.2015.02.038.
3. Thumtha C., Tawit C. (2009) Optimal angle of attack for untwisted blade wind turbine. *Renewable Energy*, 34: 1279–1284. doi:10.1016/j.renene.2008.09.017.
4. Aniket C. Aranake A, Vinod KL, Karthik D. (2015) Computational analysis of shrouded wind turbine configurations using a 3-dimensional RANS solver. *Renewable Energy*, 75: 818-832. doi:10.1016/j.renene.2014.10.049.
5. Zanotti A , Nilifard R, Gibertin G, Guardone A, Quaranta G. (2014) Assessment of 2D/3D numerical modeling for deep dynamic stall experiments. *Journal of Fluids and Structures*; 51: 97–115. doi:10.1016/j.jfluidstructs.2014.08.004.
6. Guoqing Z, Qijun Z. (2014) Parametric analyses for synthetic jet control on separation and stall over rotor airfoil. *Chinese Journal of Aeronautics*, 27(5): 1051–1061. doi:10.1016/j.cja.2014.03.023.
7. Rostamzadeh N, Hansen, KL, Kelso RM, Dally BB, (2014) The formation mechanism and impact of streamwise vortices on NACA 0021 airfoil's performance with undulating leading edge modification. *Physics of Fluids* 26(10):p1. doi:10.1063/1.4896748.
8. Mashud K, Bijoy P, Rahman N. (2014) Numerical simulation of free surface water wave for the flow around NACA 0015 hydrofoil using the volume of fluid (VOF) method. *Ocean Engineering*, 78: 89–94. doi:10.1016/j.oceaneng.2013.12.013.
9. Ladson CL. (1988) Effects of Independent Variation of Mach and Reynolds Numbers on the Low-Speed Aerodynamic Characteristics of the NACA 0012 Airfoil Section. NASA TM 4074.
10. Gregory N, and Reilly CLO. (1970) Low-Speed Aerodynamic Characteristics of NACA 0012 Aerofoil Section, including the Effects of Upper-Surface Roughness Simulating Hoar Frost. A.R.C., R. & M. No. 3726.
11. Menter FR. (1994) Two-Equation Eddy-Viscosity Turbulence Models for Engineering Applications. *AIAA Journal*, 32(8) 1598-1605.
12. <http://www.comsol.com> (2016) COMSOL CFD module user guide.